

# Testing of nonlinear diamond-turned reflexicons

John Hayes, K. L. Underwood, John S. Loomis, Robert E. Parks, and James C. Wyant

The extreme alignment sensitivity of nonlinear diamond-turned reflexicons makes them difficult to test and analyze. To evaluate the wave front it is necessary to know what portion results from alignment errors. This paper describes the setup, alignment, and testing of a nonlinear diamond-turned independent-element reflexicon manufactured at the Union Carbide, Oak Ridge Y-12 plant. Interferograms taken with the center cone misaligned a known amount are analyzed using the axicon preprocessing option in FRINGE [J. S. Loomis (ASTM Report STP 666 and Proc. Soc. Photo-Opt. Instrum. Eng. 171,64 (1979)]. The results show that FRINGE correctly removes the cone and decenter errors introduced by the misalignments. It is also shown how the resulting interferograms are unfolded to give the OPD errors as seen on the outer cone.

## I. Introduction

Axially symmetric conical optical elements are being used in high power chemical lasers to extract energy from large diameter annular gain regions with small annular thicknesses. These optical elements are generally axicons used in pairs to form either waxicon or reflexicon elements (see Fig. 1). The reflexicon, which will be discussed in this paper, consists of an inner and an outer cone both facing the same direction. Working in transmission, this arrangement converts an annular beam into a solid beam. To change the input-output beam magnification ratio, the cross-sectional surface profiles on the two cones may be nonlinear.

The two nonlinear cones are generally produced independently by single-point diamond turning. While this technique usually produces an accurate surface figure, it is desirable to use conventional polishing techniques to remove both the turning marks and any residual surface errors that will affect the final output energy distribution. It is then necessary to develop an optical testing scheme that can accurately monitor the polishing process.

Since the reflexicon itself forms an afocal system, it is in principle simple to test. However, misalignments

between the two independent elements of the reflexicon introduce errors that must be separated from the errors introduced by surface misfiguring.

This paper describes a method developed at the Optical Sciences Center to test nonlinear diamond-turned reflexicons manufactured at the Union Carbide Oak Ridge Y-12 plant. The reflexicon under test accepts a 317.5-cm diam annular beam and outputs a 177.8-cm solid beam. The parabolic cross-sectional profiles on both the inner and outer cones produce a magnification ratio of 3.0. The testing method uses careful alignment techniques to first minimize alignment errors. Any remaining errors are then removed by the axicon preprocessing option in FRINGE.<sup>1,2</sup> It is also shown how the wave front errors are mapped onto the surface of the outer cone.

## II. Alignment Errors

Figure 2 shows the four possible alignment errors in the nonlinear reflexicon in double pass. The phase errors are found by computing the optical path as a function of pupil coordinates between the misaligned surfaces of the inner and outer reflexicon cones. Multiplying the optical path errors by  $2\pi/\lambda$  gives the phase error. For small misalignments, the phase errors as a function of polar pupil coordinates are given by the following expressions<sup>3</sup>:

- (1) Off-axis illumination

$$\phi_1 = (\theta_{yb} \sin\phi - \theta_{xb} \cos\phi)a_1r;$$

- (2) Inner cone tilt

$$\phi_2 = (\theta_{yi} \sin\phi - \theta_{xi} \cos\phi)(a_2r + a_3r^2);$$

- (3) Axial inner cone displacements

$$\phi_3 = \delta_{zi}(a_4 + a_5r + a_6r^2);$$

- (4) Lateral inner cone displacement

When this work was done all authors were with University of Arizona, Optical Sciences Center, Tucson, Arizona 85721; John Loomis is now with University of Dayton Research Institute, Dayton, Ohio 45469.

Received 13 June 1980.

0003-6935/81/020235-06\$00.50/0.

© 1981 Optical Society of America.

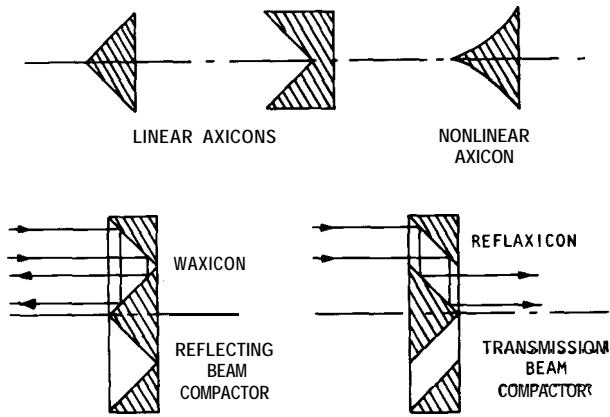


Fig. 1. Axicon optical systems.

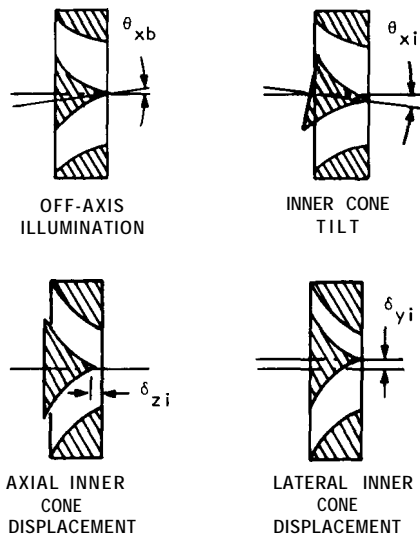


Fig. 2. The four possible alignment errors in the reflaxicon system.

$$\phi_4 = (\delta_{yi} \cos\phi + \delta_{xi} \sin\phi)(a_7 + a_8r);$$

where  $r$  = radial pupil coordinate, measured from the optical axis,

$\phi$  = azimuthal pupil coordinate, measured from the vertical  $y$  axis, and

$a_1$ - $a_8$  = constants determined by the axicon profile parameters.

The first two errors: off-axis illumination and inner cone tilt, introduce tilt fringes. This is true for inner cone tilt because the condition that  $a_2 \gg a_3$  is met for the system under test.

Phase errors introduced by the first two misalignments are fairly easily detected and corrected during alignment. A flat fiducial surface machined onto the rear surface of the outer cone makes it easy to align with the test beam. Tip and tilt of the inner cone can then be adjusted to minimize tilt fringes. Any residual tilt error can be removed in the FRINGE alignment program.

Axial displacement of the inner cone introduces a constant piston error as well as cone and focus errors. Since both the cone and focus errors produce circular fringes, it is simple to find the correct axial position of the inner cone during alignment.

The phase error introduced by a lateral displacement of the inner cone is found by computing the OPD between two laterally displaced conical surfaces. The first-order effect of decentering elements can best be seen by looking at the moiré pattern produced by the concentric equispaced circular contours of a linear cone placed on top of itself and decentered slightly. For a nonlinear cone, the circles would not be equispaced, but the basic effect of decenter for a perfect reflaxicon can be observed by using equispaced concentric circles. The resulting moiré pattern shown in Fig. 3 consists of hyperbolas. However, as long as we stay away from the center of the pattern we can consider the moiré pattern to be straight lines. It can be shown that for a given fringe making up the moiré pattern we have the condition that

$$B_1 \cos\phi + B_2 \sin\phi = \text{constant}. \quad (1)$$

$B_1$  and  $B_2$  are proportional to the lateral displacement in the  $x$  and  $y$  directions, respectively, and  $\phi$  is the angle the straight fringe makes with respect to the  $+x$  axis. Thus, if we least squares fit the interferogram data to an equation of the form of Eq. (1), we can determine both the magnitude and direction of displacement.

There is an additional phase error introduced if the large flat mirror used in the double-pass test setup is tilted. The error is given by:

$$\phi_5 = (\theta_{yf} \sin\phi - \theta_{xf} \cos\phi)(a_9 + a_{10}r),$$

where  $\theta_{yf}$ ,  $\theta_{xf}$  = tip and tilt angles of the flat; and  $a_9$ ,  $a_{10}$  = constants determined by axicon profile parameters.

It is generally not necessary to worry about this error since it is very simple to align correctly the large flat in the initial set up.

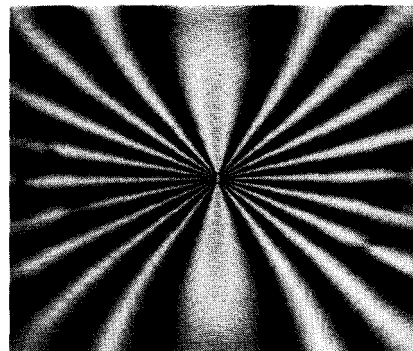


Fig. 3. Hyperbolic fringes formed by the moiré between two circular fringe patterns. This is the same aberration formed by a linear reflaxicon with a small amount of decenter between the elements.

### III. Testing Scheme

The reflexicon is being tested in double pass with a polarization Twyman-Green unequal-path interferometer. Circularly polarized light is used to eliminate any artifacts introduced into the wave front due to the phase shifts that occur at the high angle of incidence metallic surfaces in the reflexicon. Light from the beam diverger on the interferometer is collimated with a 25-cm diam collimating lens. The beam then strikes the inner cone of the reflexicon and is collimated by the outer cone. A large flat is used to return the beam back through the system to the interferometer. The setup can be seen in Figs. 4 and 5.

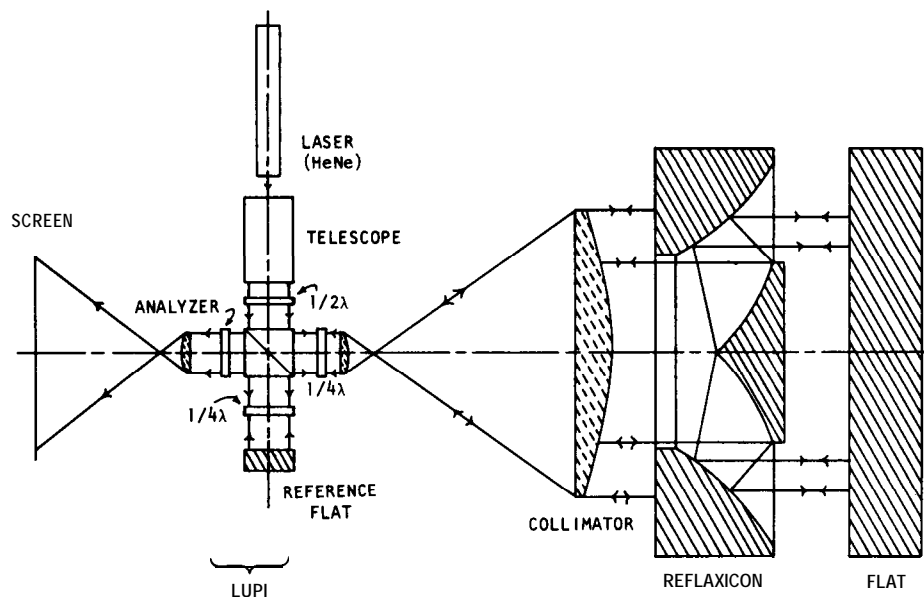


Fig. 4. Schematic diagram of the test setup.

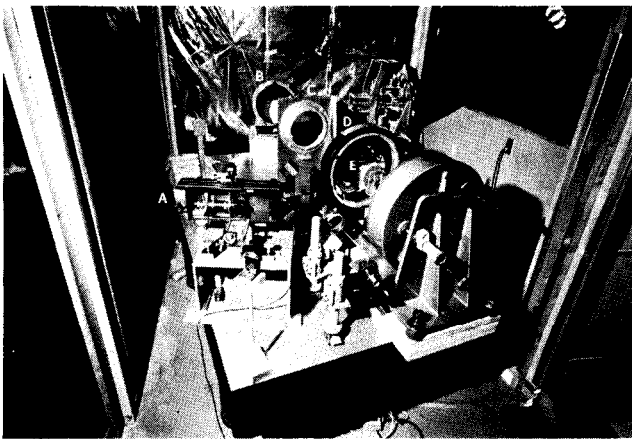


Fig. 5. The test setup: (A) Twyman-Green interferometer, (B) folding flat, (C) collimating lens, (D) reflexicon outer cone, (E) reflexicon inner cone, (F) large flat mirror.

The alignment of the system is critical to reducing the errors introduced by tilts and decenters. The interferometer is first used with a corner cube reference mirror to align the collimator and large flat for zero tilt. The outer cone is then inserted into the beam and is set to zero tilt by looking at the wave front returned off the reference surface machined onto its rear surface. It is essential that the collimating lens pass a beam larger than the hole in the outer cone for this purpose.

The initial alignment of the center cone is straight-forward. The correct axial position of the cone is found by minimizing the cone error seen in the interference pattern. Tip and tilt are controlled by minimizing the number of tilt fringes introduced by small angular dis-

placements. Minimizing the number of fringes of decenter (spoke-shaped fringes) determines the correct lateral position of the center cone. This last adjustment is the most difficult to make and is the most likely to contain errors. Since axial and angular displacements are the simplest errors to correct in the setup, FRINGE is used primarily to eliminate decentering errors.

### IV. Experimental Test of FRINGE

To test the axicon preprocessing option a simple straightforward experiment was performed. The entire optical system was set up to minimize the most easily detectable errors such as the tilt and axial displacement of the inner cone and the off-axis illumination of the entire axicon system. The inner cone was then positioned to minimize decenter fringes. A Federal model 432 electronic gauge head was used to measure inner cone decenter. Interferograms were taken at the reference position and with horizontal displacements of 2  $\mu\text{m}$ , 4  $\mu\text{m}$ , and 6  $\mu\text{m}$ . As a check, the inner cone was

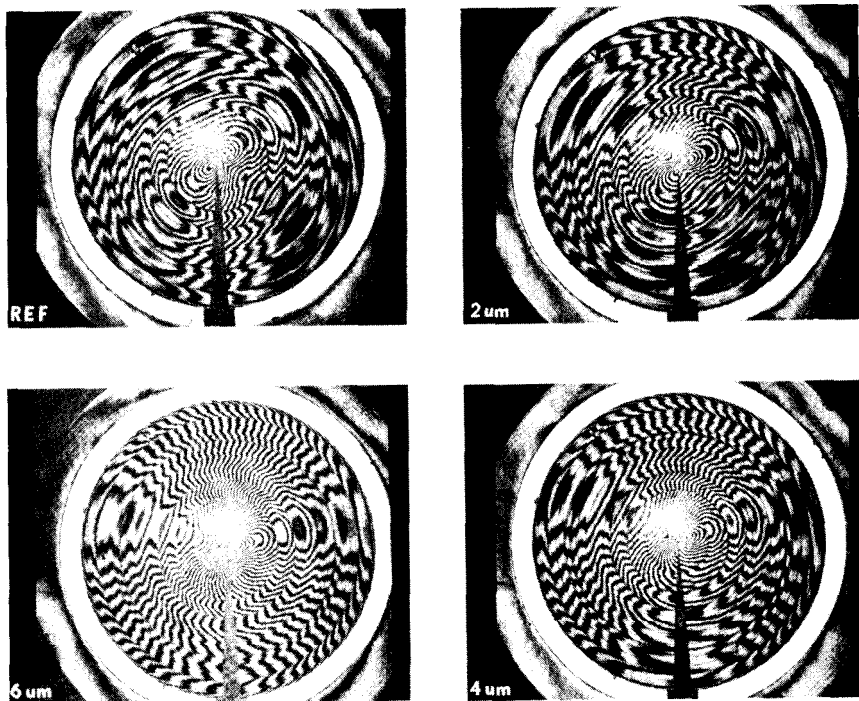


Fig. 6. Double-pass interferograms showing different amount of decenter.

returned to the initial position, as indicated by the gauge, and an interferogram was recorded. The interferograms can be seen in Fig. 6.

The interferograms were then digitized by hand on a bit pad and analyzed using the axicon preprocessing option on FRINGE. Because the interferogram of the 6- $\mu\text{m}$  displacement showed too many fringes, it was not analyzed. This is not a serious loss of data since we are interested primarily in removing the effects of small amounts of decenter. The results, which are summarized in Table I, show that the amount of decenter calculated by the axicon option is very close to the actual measured values. The most important test is that FRINGE should be able to calculate the same OPD maps regardless of the amount of decenter. Figure 7 shows the OPD maps of the interferograms, and the agreement is quite good.

## V. Unfolding the OPD Maps

To see the OPD error on the outer cone it is necessary to project the solid OPD map onto the outer cone. Figure 8 shows how this projection is done. The equation of each parabolic cross section is given by  $y = 1/4 f_x^2$ . Since the reflexicon is afocal, the coordinates of the input and output rays ( $x_1$  and  $x_2$ ) can be found by solving for equal slopes on the inner and outer axicon elements:

$$x_2 = (f_o/f_i)x_1$$

where  $f_o$  = cross-sectional focal length of outer cone and  $f_i$  = cross-sectional focal length of inner cone. The radial coordinates of each ray are then found by changing coordinates:

Table 1. Experimental Results <sup>a</sup>

	Reference <sup>b</sup>	y = 2 $\mu\text{m}$ <sup>b</sup>	y = 4 $\mu\text{m}$ <sup>b</sup>
$\delta_x$	-1.1 $\mu\text{m}$	0.6 $\mu\text{m}$	2.4 $\mu\text{m}$
$\delta_y$	-0.2 $\mu\text{m}$	-0.3 $\mu\text{m}$	-0.5 $\mu\text{m}$
Total shift	-	1.7 $\mu\text{m}$	3.5 $\mu\text{m}$

<sup>a</sup>The shift values are the measured decenter distances. The  $\delta_x$ ,  $\delta_y$  values are the positions calculated from the digitized interferograms by FRINGE. The total calculated y shifts from the initial reference position agree quite well with the measured displacements.

<sup>b</sup>Measured shift along y axis.

$$r_1 = x_0 - x_1, \quad r_2 = x_0 - x_2.$$

Finally,

$$r_2 = \frac{1}{m} r_1 + A,$$

where  $m = f_i/f_o$  = system magnification, and  $A = x_o(1 - f_o/f_i)$ . FRINGE has been modified to show the OPD maps on the outer cone as well as the inner cone. An unfolded OPD contour map is shown in Fig. 9.

## VI. Conclusion

This paper has described a method of testing nonlinear independent-element reflexicons using computer processing to remove errors introduced by misalignments. The results of an experimental test of the method clearly show that FRINGE is able to correctly remove the alignment errors from the wave front under test. This testing method is now being used at the Optical Sciences Center and has proved to be quite satisfactory.

This work was supported by the United States Air Force, Air Force Weapons Laboratory, Kirtland Air Force Base, New Mexico.

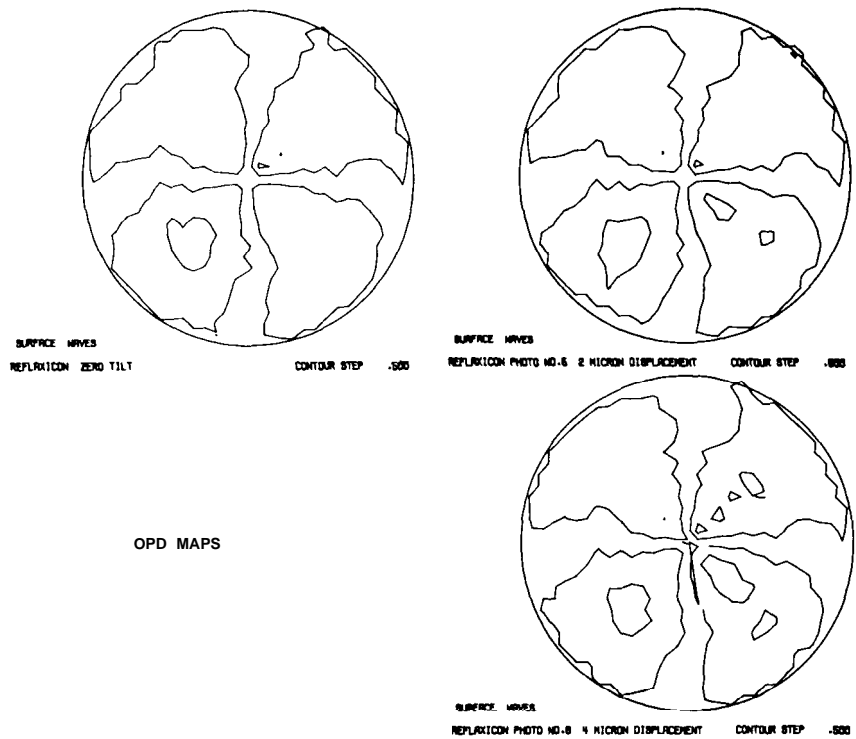


Fig. 7. OPD maps generated from the interferograms.

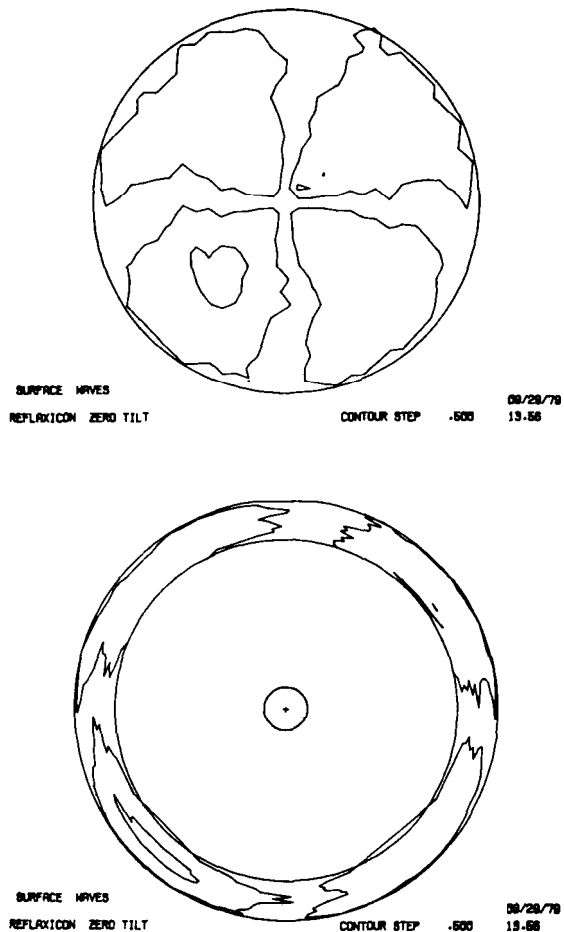


Fig. 9. OPD maps as seen at the solid output (top) and on the outer cone (bottom).

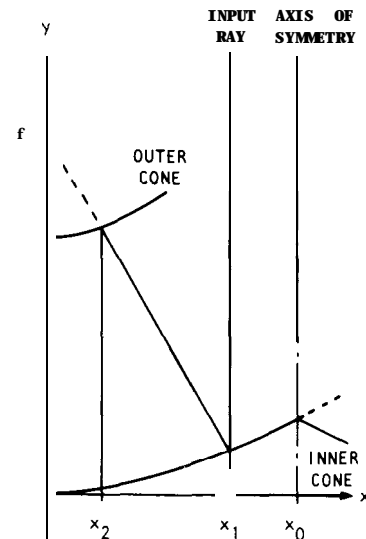


Fig. 8. Geometry used to unfold the OPD maps to show the surface errors on the outer cone.

### References

1. J. S. Loomis, "A Computer Program for Analysis of Interferometric Data," in *Optical interferograms-Reduction and Interpretation* (American Society for Testing and Materials, Philadelphia, 1978), ASTM STP 666, A. H. Guenther and D. H. Liebenberg, Eds., pp. 71-86.
2. J. S. Loomis, Proc. Soc. Photo-Opt. Instrum. Eng. 171, 64 (1979).
3. P. W. Scott, Rocketdyne Division of Rockwell International, Internal Letter No. G-0-79-2062, 1 Mar. 1979.